

Evolutionary-Optimized Photonic Network Structure in White Beetle Wing Scales

Bodo D. Wilts^{#,*}, Xiaoyuan Sheng^{*}, Mirko Holler, Ana Diaz, Manuel Guizar-Sicairos, Jörg Raabe, Robert Hoppe, Shu-Hao Liu, Richard Langford, Olimpia D. Onelli, Duyu Chen, Salvatore Torquato, Ullrich Steiner, Christian G. Schroer, Silvia Vignolini, and Alessandro Sepe[#]

Whiteness arises from the random scattering of incident light from disordered structures.^[1] Opaque white materials have to contain a sufficiently large number of scatterers and therefore usually require thicker, material-rich nanostructures than structural color arising from the coherent interference of light.^[2,3] In nature, bright white appearance arises from the dense arrays of pterin pigments in pierid butterflies,^[4] guanine crystals in spiders,^[5] or leucophore cells in the flexible skin of cuttlefish.^[6] A striking example of such whiteness is found in the chitinous networks of white beetles, e.g. *Lepidiota stigma* and *Cyphochilus sp.*^[7–9] Previous research investigating these beetle structures has shown that the chitinous network is one of the most strongly scattering materials in nature and therefore the question arises whether this structure is evolutionary optimized for strong scattering whilst minimizing the amount of employed material, thus reducing the weight of the organism. The brilliant white reflection from *Cyphochilus* beetles is assumed to be important for camouflage among white fungi and in a shady environment.

In contrast to periodic photonic materials, for which the optical response is straightforward to calculate, the reflection of light from such disordered network morphologies requires a detailed knowledge of local geometry.^[2,3,9,10] For these complex cases, the validity

Dr. B. D. Wilts, X. Sheng, Prof. U. Steiner, Dr. A. Sepe
Adolphe Merkle Institute, Chemin des Verdiers, 1700 Fribourg, CH
[#]e-mail: bodo.wilts@unifr.ch, alessandro.sepe@unifr.ch

* Contributed equally.

Dr. M. Holler, Dr. A. Diaz, Dr. M. Guizar-Sicairos, Dr. Jörg Raabe
Swiss Light Source, Paul Scherrer Institute, 5232 Villigen, CH

R. Hoppe
Institute of Structural Physics, Technische Universität Dresden,
10162 Dresden, Germany

X. Sheng, S.-H. Liu, Dr. R. Langford
Department of Physics, University of Cambridge, JJ Thompson Avenue,
CB3 0HE Cambridge, UK

O. D. Onelli, Dr. S. Vignolini
Department of Chemistry, University of Cambridge, Lensfield Road,
CB2 1EW Cambridge, UK

D. Chen, Prof. S. Torquato
Department of Chemistry, Princeton University, Princeton, NJ
08544, USA

Prof. C. G. Schroer
Deutsches Elektronen-Synchrotron DESY, Notkestr. 85, 22607
Hamburg, Germany and Department of Physics, Universität Ham-
burg, Luruper Chaussee 149, 22761 Hamburg, Germany

of the diffusion approximation is limited, since single scattering elements are difficult to be identified.^[7] To fully understand the correlation between the structure and (optical) properties of complex materials, the detailed real-space structure in combination with a suitable model unravels this relationship. In optics, these include finite-element modeling (FEM) or finite-difference time-domain (FDTD) techniques, which can be employed for materials with arbitrary structures.^[11]

Distortion-free three-dimensional imaging of biological tissue with sub-micrometer resolution in a large volume is cumbersome and often relies on destructive techniques, i.e. FIB-SEM serial tomography or electron tomography.^[7,12] Multi-keV ptychographic X-ray computed tomography (PXCT)^[13] overcomes this limitation, achieving below 15 nm resolution in radiation-hard materials at room temperature.^[14] In radiation-sensitive materials, however, the PXCT resolution used to be much worse (> 100 nm), limited by either radiation damage at room temperature or by drifts of the setup at cryogenic temperatures.^[15,16] Here, we use “OMNY” (“tOMography Nano crYo”, see SI), an instrument that allows cryo-PXCT of biological materials, overcoming these imaging limitation. Cryogenic conditions preserve the structure of the sample during the measurement time, and interferometric positioning control eliminates thermal drifts.^[17] We use OMNY to image single wing scales of the brilliant white beetle *Cyphochilus sp.* These measurements provide a full structural characterization of the network morphology within the scales, clearly demonstrating the power of cryo-PXCT to extract quantitative structural information from biological tissues in a non-invasive, damage-resistant fashion.

Cyphochilus beetles (Coleoptera: Scarabaeidae: Melolonthinae) occur widely across Southeast Asia. The entire exoskeleton of the beetle (**Figure 1a**) is patterned with single wing scales covering the else velvet black exocuticle, which can be clearly seen by optical microscopy (**Figure 1b**). Each scale spans approximately 200 μm in length and 60 μm in width. These scales strongly scatter incident light and the reflectance is more or less constant across the visible wavelength range (**Figure S3** and^[7]).

Closer inspection of the white scales using scanning electron microscopy (SEM) reveals that the scale interior comprises a network of interconnected, chitinous fibres surrounded by air.^[7–9,18,19] Earlier interpreta-

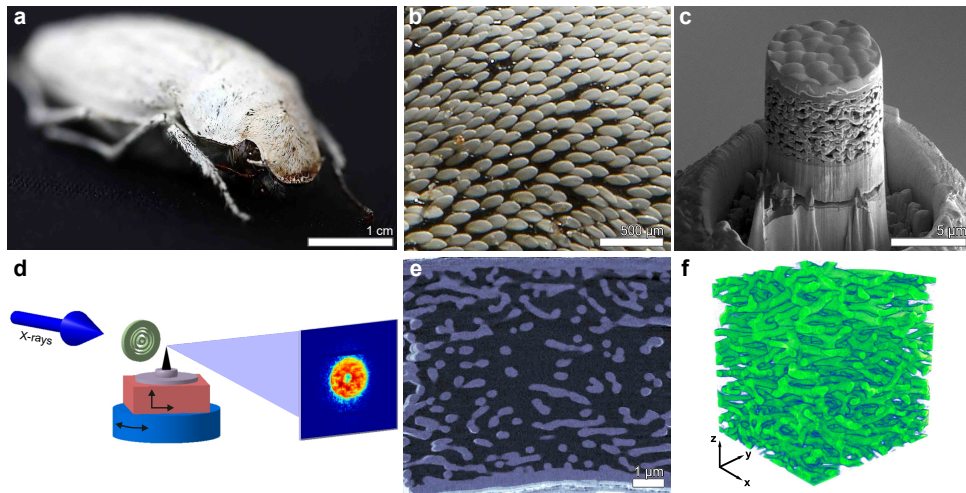


Figure 1: The brilliant white beetle *Cyphochilus* sp. (a) Macro photograph. (b) Light micrograph of the scale arrangement on the beetle’s elytra. (c) Scanning electron micrograph of the sample pillar on a nanotomography pin-holder obtained from a beetle scale by focused ion-beam milling. (d) Sketch of the X-ray nanotomography setup. The sample is scanned and rotated through the beam (indicated by arrows) while recording the diffraction pattern (see SI for more details). (e) High-resolution tomographic slice (see movies **S2**, **S3**) and (f) 3D reconstruction of a $7 \times 7 \times 7 \mu\text{m}^3$ inset of the volume obtained by cryo-PXCT of the inner structure of a beetle wing scale.

tions of the optical response of the scales^[7,9] was hampered by the lack of artifact-free, three-dimensional visualisation of the complex chitinous cuticle structure, and claims concerning the evolutionary optimized white color of the beetle were therefore anecdotal.

To gain insight into the optical function of the scales, we investigated the wing scales using PXCT. A first attempt was aimed at reconstructing the network morphology inside the beetle scale using conventional room-temperature PXCT,^[20] achieving a 3D resolution of 70 nm. Significant sample deformation was observed by visually comparing projections recorded at the beginning and end of the PXCT measurement at the same projection angle.

To overcome this critical issue, the nanotomography measurements were repeated, using another beetle scale, at 92 K. Cryogenic conditions dramatically reduced structural deformation caused by the measurement (see SI), enabling an isotropic 3D resolution of 28 nm over a sample volume of $\approx 350 \mu\text{m}^3$, which hinges on the minimization of in-situ sample deformation, a typical problem for organic materials. While still somewhat worse than that of other techniques, e.g. serial transverse sectioning and imaging using transmission electron microscopy or X-ray crystallography, cryo-PXCT is non-invasive and does not rely on complicated embedding and/or staining protocols.

The spectral properties of the beetles are particularly interesting as they provide a very efficient incoherent broad-band reflector with a comparable whiteness of common white paper but with a thickness of only about 1/10 of a typical paper sheet.^[7–9,19] To understand the key parameters governing this unusually strong scattering strength, the rendered 3D network of Figure 1f can be directly used to perform FDTD simulations of the structure’s optical response to incident white light. The strength of this approach lies i.e. in the ability to digitally modify the network morphology displayed in Figure 1f to test the changes in optical

reflectivity.

The FDTD modeling results, **Figure 2a**, show that the reflectance strongly depends on the orientation of the network volume. The reflectance is significantly higher for the typical orientation of the scale (in-plane) and reaches a peak reflectance of ≈ 0.65 , while orientations perpendicular (out-of-plane) to the scale normal are significantly less reflective, with reflectances of ≈ 0.5 . This confirms previous results by Cortese *et al.*,^[8] which showed that the time-of-flight of a laser pulse through the structure is strongly anisotropic.

To further elucidate the nature of the optical anisotropy and its possible function, the network structure was digitally stretched and compressed. Figure 2b shows that compression along the z -axis lowers the in-plane reflectance. Stretching of the structure, i.e. making it more isotropic, results only in a slightly increased reflectance (0.69 *vs.* 0.65). This indicates that the scales’ structural anisotropy reduces the thickness needed to produce strong scattering resulting in the observed brilliant whiteness. The scale thickness is functionally important for flying insects, as larger structures embedded on the wing require more material along the elytra.

By affinely expanding or contracting the network morphology, it is possible to test whether the scale structure has an optimized volume distribution of scatterers that maximize broadband reflectivity (Figure 2c). Uniform compression along all spatial directions results in a severe reduction of the reflectivity, which eventually (below 20% of the original size) disappears all together, i.e. the material becomes transparent. This result is unsurprising since for a distribution of scattering centers that is comparable to the incident wavelength, propagating light “averages” over its discrete structure, entering the “optical crowding” or “effective medium” regime.^[21] Uniform expansion of the network morphology changes the broad-band reflectance very little. This result again indicates that

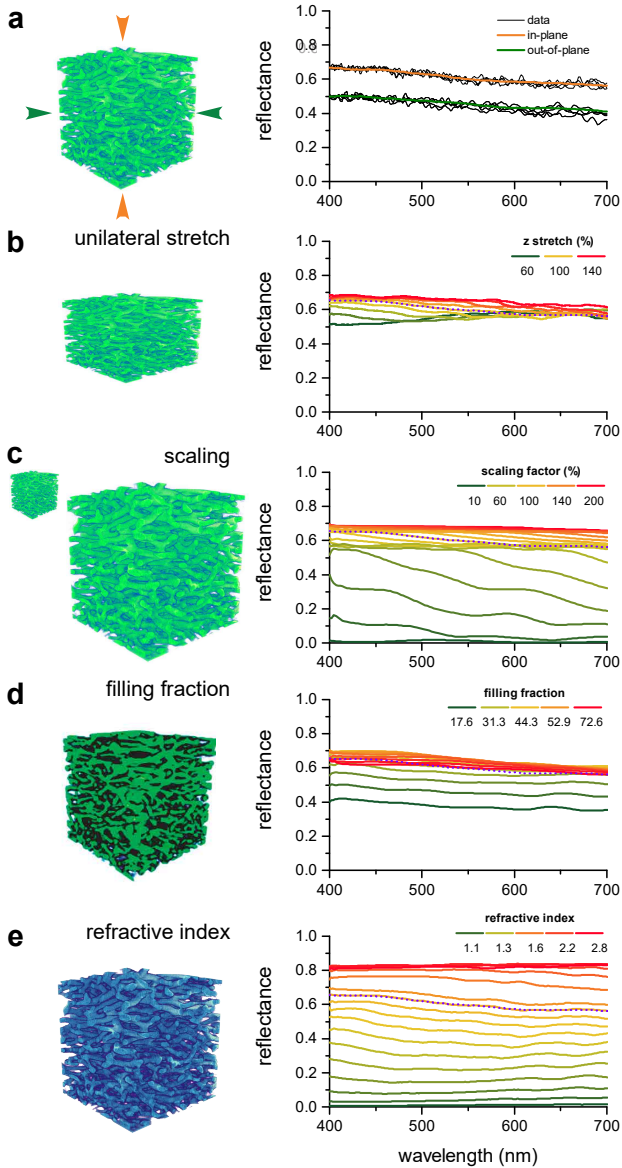


Figure 2: Spectrally resolved finite-difference time-domain (FDTD) simulations of light reflection (right column) from the network morphologies shown in the left column. (a) Comparison of in-plane and out-of-plane optical directions of the cryo-PXCT-determined morphology (Figure 1f). Reflectance as a function of (b) unidirectional stretching/compression of the structure along the z -axis; (c) affine scaling of the network; (d) filling fraction of the network struts; (e) refractive index of the material comprising the network. The dotted lines correspond to the cryo-PXCT determined structure of Figure 1f for the (common) in-plane orientation.

the structure is optimized for achieving maximal whiteness for a minimal scale thickness.

The weight of the scale is also affected by the porosity of the network morphology and therefore the strut thickness. The reconstructed morphology of Figure 1f has a solid content (filling fraction) of $45 \pm 6\%$. Figure 2d explores the optical response of the network morphology upon digitally enlarging and reducing the strut diameter, which alters the filling fraction. Optimal broad-band reflection was found for a rather broad filling-fraction range, from ~ 40 – 70% . The filling fraction of the beetle scales of $\approx 45\%$ lies at the lower end of this range, again indicating an optimization that maximizes scattering power for a minimum of material

use.

Fundamentally, the scattering power in single and multiple scattering systems depends strongly on the refractive index. While biological organisms have limited access to high refractive index materials, it is interesting to explore the variation of the network reflectivity for different, synthetically-available refractive indices. In Figure 2e, the refractive index was varied from $n = 1.1$ to 2.8 , where the void-space of the network was modeled as air with $n_{\text{air}} = 1$. While, unsurprisingly, higher refractive indices result in a stronger average reflectance, up to 84% for $n = 2.8$ (i.e. close to that of rutile titanium dioxide, a synthetic dielectric material commonly employed in photonic applications^[22]), the broad-band reflectivity rapidly decays for $n < 1.6$. Given the fact that the refractive index of chitin, varying from 1.6 to 1.55 (blue to red wavelengths, respectively), is among the highest found for purely organic biological materials,^[23,24] this simulation illustrates yet another aspect of optical optimization of the network morphology.

The careful balance of structural parameters described above begets the question whether the random network morphology exhibits hidden correlations that optimize the scattering of incident light. This question is motivated by the consideration that the optimization of the scattering strength requires an average distance between scatterers just above the wavelength of visible light (to avoid optical crowding) and the absence of periodic order (to avoid a photonic band-gap,^[25,26]). An established example of such hidden correlations is “hyperuniformity”, which refers to the anomalous suppression of density fluctuations at large length scales.^[27–29] Hyperuniform systems include all perfect spatially periodic patterns, and special disordered systems. To date, disordered hyperuniformity has been discovered in only a small number of biological and physical systems,^[28] including the arrangement of color sensing photoreceptors in avian retinae^[30] and designed two-dimensional photonic materials.^[29]

The high resolution cryo-PXCT data of Figure 1f enables a direct structural analysis and to test the data for hidden correlations. Using a medial axis analysis,^[31] the distribution of lengths and width of the individual struts forming the network structure was analyzed (Figure 3a-c). Both parameters show very broad distributions of 1105 ± 360 nm (mean \pm full-width-at-half-maximum) and 115 ± 80 nm, respectively, which is typical for random network structures.

To investigate whether this seemingly random morphology has hidden structural correlations, e.g. hyperuniformity, the spectral density χ_k in the various planes of the Fourier space of the network structure was calculated. The scaled spectral density profile along the two main directions (out-of- and in-plane of the beetle scale) are shown in Figure 3d,e. The density profile is strongly dependent on the direction of investigation indicating a strong structural anisotropy of the network (c.f. Figure 1b). While the spectral densities in the two out-of-plane directions, x - z and y - z , show strong directional dependence (Figure 3d), the spec-

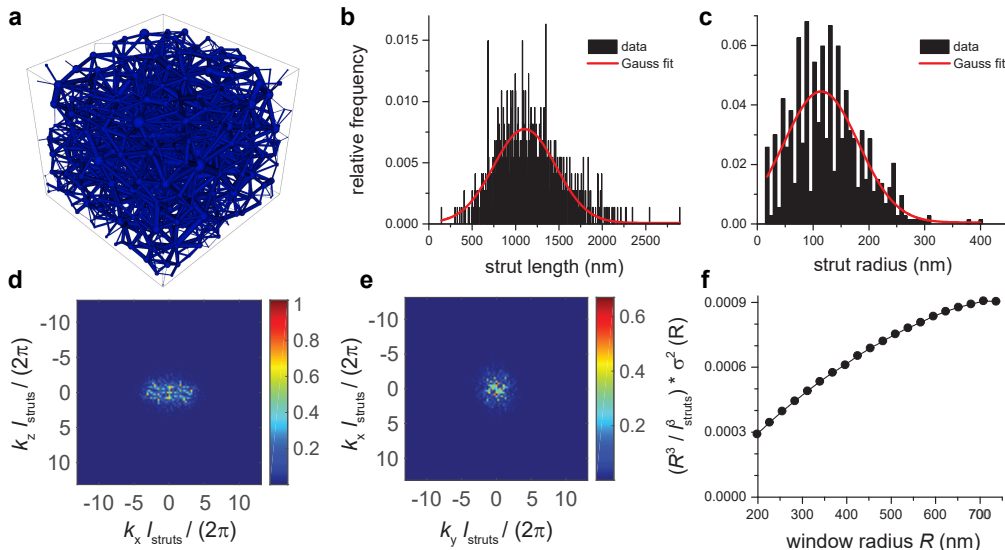


Figure 3: Structural analysis of the reconstructed photonic structure. (a) Sketch of the medial axis representation of the network. (b,c) Size statistics of the strut length (b) and width (c), respectively. (d,e) Scaled spectral density $\tilde{\chi}_k$ of the network along two characteristic planes in the Fourier space parallel (d) and perpendicular (e) to the structure normal. (f) Scaled local volume fraction as a function of the window radius R . In this representation a linear decay for $R \rightarrow 0$ is indicative of a random distribution.

tral density in the in-plane direction, x - y , is largely isotropic (Figure 3e). Along the out-of-plane direction the structure seems to be "layer-like" with a pseudo-layer distance of ≈ 270 nm. The anisotropy of the nanostructure can be further quantified by the quantity $\xi = \frac{\tilde{\chi}(0,0,k_z \rightarrow 0)}{\tilde{\chi}(k_x \rightarrow 0, k_y \rightarrow 0, 0)} - 1$, where $\tilde{\chi}(0,0,k_z \rightarrow 0)$, and $\tilde{\chi}(k_x \rightarrow 0, k_y \rightarrow 0, 0)$ are extrapolated values of the spectral density in the z direction and x - y plane as \mathbf{k} approaches 0 and $\tilde{\chi}(k_x, k_y, k_z) \equiv \tilde{\chi}(\mathbf{k})$. For isotropic structures, ξ should be 0 and increase for increasing structural anisotropy. In the case of the investigated structure, ξ is in the order of 10, indicating a strong structural anisotropy. Figures 3d,e moreover illustrate that the network morphology is not strictly hyperuniform, since $\tilde{\chi}_k$ does not vanish as the wavenumber k approaches 0 from any direction. This fact is further corroborated by investigating the local variation of the volume fraction of scatterers as a function of a spherical probe of radius R . Figure 3f shows that the scaled local volume fraction variance $R^3 \sigma^2(R)$ varies linearly with R and plateaus for large R . Hyperuniformity requires a faster decay for $R \rightarrow 0$.^[28,32] The results of Figure 3 therefore clearly demonstrate the absence of hyperuniformity and the two size distributions of Figure 3b,c are close to Gaussian. In addition, we have employed a variety of other structural descriptors to spatially characterize the beetle ultrastructure, as detailed in the Supporting Information.

In summary, we have employed a new experimental technique, cryo-PXCT, to study the nanostructured photonic system of the *Cyphochilus* beetle. The combination of cryo-PXCT structural reconstruction with sub-30 nm resolution with FDTD modeling allowed to demonstrate that the 3D network morphology of the beetle is carefully optimized by evolution. This is achieved by the judicious simultaneous selection of 4 parameters, the selection of (1) the correct network

density, (2) the optimal fill fraction, (3) one of the biologically highest refractive indices for transparent materials, and (4) a beneficial structural anisotropy. Changing any of these parameters may improve one of the decisive properties (e.g. reflectivity), but always at the expense of the other (e.g. used material per unit area). In particular, the digital variation of these 4 network parameters in Figure 2 does confirm the optimized nature of the photonic network morphology, that maximizes the white broad-band reflectivity while minimizing the materials use (and hence weight) per unit area.

Metabolically the production of the wing scale material is considerable, given its relatively large thickness of ≥ 7 μm . Each beetle wing scale, similar to the wing scales of butterflies, develops from a single differentiating cell,^[33] most likely through pre-stretching of internal F-actin filaments and subsequent external deposition of chitinous cuticle. Three-dimensional structures in arthropods are often highly ordered (see e.g.^[26,34,35]) and the precise mechanism driving structure formation is still an open debate. While some work exists on periodic morphologies in butterfly wing scales,^[33,35] structure formation of disordered networks in developing wing scale cells is up to now uninvestigated.

While the optimization of materials use is evidently essential for flying insects, it presents a bio-inspired design strategy for the manufacture of white reflectors, particularly in applications in which the use of low refractive index organic materials is desirable, e.g. the food industry. Additionally, the use of higher refractive index materials allows to even further improve the scattering strength of similar network materials while minimizing materials use and weight of the coating.

Supporting Information

Supporting Information is available from the Wiley Online Library or from the author.

Acknowledgements

We thank Frank Scheffold, Andreas Menzel and Oliver Bunk for fruitful discussions, Demet Asil, Reza Saberi Moghaddam, Eric Tapley and Jon J. Rickard for help with experiments, Charly Rappo for the permission to use the photograph of Figure 1a, Holger Averdunk for help with the medial axis representation. The OMNY instrumentation was supported by the Swiss National Science Foundation SNSF (Funding scheme RQUIP, Project number 145056). This research was financially supported through the National Centre of Competence in Research *Bio-Inspired Materials*, the Adolphe Merkle Foundation and the Ambizione program of the Swiss National Science Foundation SNSF (168223, to BDW). We acknowledge the support from the Winton Programme for the Physics of Sustainability.

Author Contributions

BDW, US, AS and SV conceived the research project. XS, S-HL, RL, ODO and SV prepared the samples. XS, MH, AD, MG-S, JR, RH, CS, and AS participated in the X-ray experiments. AD and MG-S analyzed the X-ray data towards 3D reconstructions. BDW performed FDTD simulations. DC, BDW and ST performed statistical analysis of the structure. BDW, US, and AS wrote the paper with contributions from all authors.

-
- [1] D. S. Wiersma. *Nat. Photonics* **2013**, *7*, 3 188.
 - [2] M. Srinivasarao. *Chem. Rev.* **1999**, *99*, 7 1935.
 - [3] S. Kinoshita, S. Yoshioka, J. Miyazaki. *Rep. Prog. Phys.* **2008**, *71*, 7 076401.
 - [4] B. D. Wilts, B. Wijnen, H. L. Leertouwer, U. Steiner, D. G. Stavenga. *Adv. Opt. Mater.* **2017**, *5* 1600879.
 - [5] A. Levy-Lior, E. Shimon, O. Schwartz, E. Gavish-Regev, D. Oron, G. Oxford, S. Weiner, L. Addadi. *Adv. Funct. Mater.* **2010**, *20*, 2 320.
 - [6] L. M. Mähger, S. L. Senft, M. Gao, S. Karaveli, G. R. R. Bell, R. Zia, A. M. Kuzirian, P. B. Dennis, W. J. Crookes-Goodson, R. R. Naik, G. W. Kattawar, R. T. Hanlon. *Adv. Funct. Mater.* **2013**, *23*, 32 3980.
 - [7] M. Burreli, L. Cortese, L. Pattelli, M. Kolle, P. Vukusic, D. S. Wiersma, U. Steiner, S. Vignolini. *Sci. Rep.* **2014**, *4* 6075.
 - [8] L. Cortese, L. Pattelli, F. Utel, S. Vignolini, M. Burreli, D. S. Wiersma. *Adv. Opt. Mater.* **2015**, *3*, 10 1337.
 - [9] P. Vukusic, B. Hallam, J. Noyes. *Science* **2007**, *315* 348.
 - [10] S. Vignolini, T. Gregory, M. Kolle, A. Lethbridge, E. Moryrou, U. Steiner, B. J. Glover, P. Vukusic, P. J. Rudall. *J. R. Soc. Interface* **2016**, *13*, 124 20160645.
 - [11] B. D. Wilts, K. Michielsen, H. De Raedt, D. G. Stavenga. *Proc. Natl. Acad. Sci. U.S.A.* **2014**, *11*, 12 4363.
 - [12] J. W. Galusha, L. R. Richey, J. S. Gardner, J. N. Cha, M. H. Bartl. *Phys. Rev. E* **2008**, *77*, 5 050904.
 - [13] M. Dierolf, A. Menzel, P. Thibault, P. Schneider, C. M. Kewish, R. Wepf, O. Bunk, F. Pfeiffer. *Nature* **2010**, *467*, 7314 436.
 - [14] M. Holler, M. Guizar-Sicairos, E. H. Tsai, R. Dinapoli, E. Müller, O. Bunk, J. Raabe, G. Aeppli. *Nature* **2017**, *543*, 7645 402.
 - [15] A. Diaz, B. Malkova, M. Holler, M. Guizar-Sicairos, E. Lima, V. Panneels, G. Pigino, A. G. Bittermann, L. Wettstein, T. Tomizaki, et al. *J. Struct. Biol.* **2015**, *192*, 3 461.
 - [16] E. Lima, A. Diaz, M. Guizar-Sicairos, S. Gorelick, P. Perrot, T. Schleier, A. Menzel. *J. Microsc.* **2013**, *249*, 1 1.
 - [17] M. Holler, J. Raabe. *Opt. Eng.* **2015**, *54*, 5 054101.
 - [18] B. T. Hallam, A. G. Hiorns, P. Vukusic. *Appl. Opt.* **2009**, *48*, 17 3243.
 - [19] S. M. Luke, B. T. Hallam, P. Vukusic. *Appl. Opt.* **2010**, *49*, 22 4246.
 - [20] M. Holler, A. Diaz, M. Guizar-Sicairos, P. Karvinen, E. Färm, E. Härkönen, M. Ritala, A. Menzel, J. Raabe, O. Bunk, et al. *Sci. Rep.* **2014**, *4*, 3857 10.
 - [21] D. J. Bergman, D. Stroud. *Solid State Phys.* **1992**, *46* 147.
 - [22] X. Chen, S. S. Mao. *Chem. Rev.* **2007**, *107*, 7 2891.
 - [23] D. E. Azofeifa, H. J. Arguedas, W. E. Vargas. *Opt. Mater.* **2012**, *35*, 2 175 .
 - [24] H. L. Leertouwer, B. D. Wilts, D. G. Stavenga. *Opt. Express* **2011**, *19*, 24 24061.
 - [25] S. R. Sellers, W. Man, S. Sahba, M. Florescu. *Nat. Commun.* **2017**, *8* 14439.
 - [26] B. D. Wilts, K. Michielsen, H. De Raedt, D. G. Stavenga. *J. R. Soc. Interface* **2012**, *9*, 72 1609.
 - [27] S. Torquato, F. H. Stillinger. *Phys. Rev. E* **2003**, *68*, 4 041113.
 - [28] S. Torquato. *Phys. Rev. E* **2016**, *94*, 2 022122.
 - [29] M. Florescu, S. Torquato, P. J. Steinhardt. *Proc. Natl. Acad. Sci. U.S.A.* **2009**, *106*, 49 20658.
 - [30] Y. Jiao, T. Lau, H. Hatzikirou, M. Meyer-Hermann, J. C. Corbo, S. Torquato. *Phys. Rev. E* **2014**, *89*, 2 022721.
 - [31] A. Jones, A. Sheppard, R. Sok, C. Arns, A. Limaye, H. Averdunk, A. Brandwood, A. Sakellariou, T. Senden, B. Milthorpe, et al. *Physica A* **2004**, *339*, 1 125.
 - [32] S. Torquato, G. Zhang, F. Stillinger. *Phys. Rev. X* **2015**, *5*, 2 021020.
 - [33] H. Ghiradella. *J. Morphol.* **1989**, *202*, 1 69.
 - [34] V. Saranathan, A. E. Seago, A. Sandy, S. Narayanan, S. G. J. Mochrie, E. R. Dufresne, H. Cao, C. O. Osuji, R. O. Prum. *Nano Lett.* **2015**, *15*, 6 3735.
 - [35] B. D. Wilts, B. A. Zubiri, M. A. Klatt, B. Butz, M. G. Fischer, S. T. Kelly, E. Spiecker, U. Steiner, G. E. Schröder-Turk. *Sci. Adv.* **2017**, *3*, 4 e1603119.
 - [36] M. Holler, J. Raabe, A. Diaz, M. Guizar-Sicairos, C. Quitmann, A. Menzel, O. Bunk. *Rev. Sci. Instrum.* **2012**, *83*, 7 073703.
 - [37] M. Guizar-Sicairos, I. Johnson, A. Diaz, M. Holler, P. Karvinen, H.-C. Stadler, R. Dinapoli, O. Bunk, A. Menzel. *Opt. Express* **2014**, *22*, 12 14859.
 - [38] P. Thibault, M. Dierolf, A. Menzel, O. Bunk, C. David, F. Pfeiffer. *Science* **2008**, *321*, 5887 379.
 - [39] P. Thibault, M. Guizar-Sicairos. *New J. Phys.* **2012**, *14*, 6 063004.
 - [40] M. Guizar-Sicairos, A. Diaz, M. Holler, M. S. Lucas, A. Menzel, R. A. Wepf, O. Bunk. *Opt. Express* **2011**, *19*, 22 21345.
 - [41] M. Guizar-Sicairos, J. J. Boon, K. Mader, A. Diaz, A. Menzel, O. Bunk. *Optica* **2015**, *2*, 3 259.
 - [42] M. Van Heel, M. Schatz. *J. Struct. Biol.* **2005**, *151*, 3 250.